Climate change scenarios of surface solar radiation in data sparse regions: a case study in Malaprabha River Basin, India

5 authors, including:

Some of the authors of this publication are also working on these related projects:

Microwave Satellite data for Soil Moisture Monitoring View project

Monsoon Mission View project

Climate change scenarios of surface solar radiation in data sparse regions: a case study in Malaprabha River Basin, India

Aavudai Anandhi[1,6], V. V. Srinivas[1], D. Nagesh Kumar[1,2,*], Ravi S. Nanjundiah[3,4], Prasanna H. Gowda[5]

[1]Department of Civil Engineering, Indian Institute of Science, Bangalore 560 012, India
[2]Center for Earth Sciences, Indian Institute of Science, Bangalore 560 012, India
[3]Centre for Atmospheric & Oceanic Sciences, Indian Institute of Science, Bangalore 560012, India
[4]Divecha Centre for Climate Change, Indian Institute of Science, Bangalore 560012, India
[5]USDA-ARS Conservation & Production Research Laboratory, Bushland, Texas 79012, USA

[6]*Present address:* Department of Agronomy, Kansas State University, Manhattan, Kansas 66506, USA

ABSTRACT: A variety of methods are available to estimate future solar radiation (SR) scenarios at spatial scales that are appropriate for local climate change impact assessment. However, there are no clear guidelines available in the literature to decide which methodologies are most suitable for different applications. Three methodologies to guide the estimation of SR are discussed in this study, namely: Case 1: SR is measured, Case 2: SR is measured but sparse and Case 3: SR is not measured. In Case 1, future SR scenarios are derived using several downscaling methodologies that transfer the simulated large-scale information of global climate models to a local scale (measurements). In Case 2, the SR was first estimated at the local scale for a longer time period using sparse measured records, and then future scenarios were derived using several downscaling methodologies. In Case 3: the SR was first estimated at a regional scale for a longer time period using complete or sparse measured records of SR from which SR at the local scale was estimated. Finally, the future scenarios were derived using several downscaling methodologies. The lack of observed SR data, especially in developing countries, has hindered various climate change impact studies. Hence, this was further elaborated by applying the Case 3 methodology to a semi-arid Malaprabha reservoir catchment in southern India. A support vector machine was used in downscaling SR. Future monthly scenarios of SR were estimated from simulations of third-generation Canadian General Circulation Model (CGCM3) for various SRES emission scenarios (A1B, A2, B1, and COMMIT). Results indicated a projected decrease of 0.4 to 12.2 W m^{-2} yr^{-1} in SR during the period 2001–2100 across the 4 scenarios. SR was calculated using the modified Hargreaves method. The decreasing trends for the future were in agreement with the simulations of SR from the CGCM3 model directly obtained for the 4 scenarios.

KEY WORDS: Downscaling · Modified Hargreaves and Donatelli-Bellocchi methods · Support vector machine · SVM · IPCC SRES scenarios · Cloud cover downscaling

1. INTRODUCTION

Solar radiation (SR; see Table 1 for further abbreviations) plays an important role in hydrological, ecological, biological, and physical processes (Rivington et al. 2005, Biggs et al. 2007, Teuling et al. 2009, Wild 2009). The lack of observed SR data, especially in developing countries, has hindered various climate change impact studies in agricultural and hydrological sectors (Iizumi et al. 2012), thus indicating a need

Table 1. Abbreviations

ANN	Artificial neural networks
C	Penalty term
CC	Cloud cover
CCCma	Canadian Center for Climate Modeling and Analysis
CFM	Change factor methodology
CGCM3	Third-generation Canadian general circulation model
CP	Solar radiation estimated using calibrated parameters
DB	Donatelli-Bellocchi method
DM	Delta change factor methodology
GCM	Global climate model
GrADS	Grid analysis and display system
IPCC	Intergovernmental Panel on Climate Change
LH	Latent heat flux
LWR	Long-wave radiation flux
MC	Malaprabha reservoir catchment
MH	Modified Hargreaves method
MRB	Malaprabha River basin
NCEP	National Centers for Environmental Prediction
NMSE	Normalized mean square error
PC	Principal component
PCA	Principal component analysis
Pptn-oc	Precipitation occurrence
PRW	Precipitable water
RBF	Radial basis function
RCM	Regional climate model
RMSE	Root mean square error
SD	Standard deviation
SH	Sensible heat flux
Sh	Sunshine hours
SR	Solar radiation
SRB	Surface radiation budget
SRES	Special report on emission scenarios
SVM	Support vector machine
SWR	Short wave radiation flux
SW_{TOA}	Extra-terrestrial radiation
Ta 925	Air temperature at 925 mb pressure level
Tave	Average temperature
Tmax	Maximum air temperature
Tmin	Minimum air temperature
T_{ng}	Threshold for correlation between predictor variables in NCEP and GCM datasets
T_{np}	Threshold for correlation between predictor variables in NCEP and predictand datasets
Ua 925	Zonal wind velocities at 925 mb pressure level
Va 925	Meridional wind velocities at 925 mb pressure level

to estimate future scenarios of SR in situations where observed SR data are sparse. Further, there are no clear guidelines to derive future SR scenarios in situations where SR data are either measured but sparse or not measured. The purpose of this paper is to shed some light on the different methods of estimating future SR scenarios under different circumstances, and to provide guidance on how they could be ap-

plied. Furthermore, one methodology is discussed in detail, using the Malaprabha River basin (MRB) in southern India as a case study.

Based on the availability of measured SR data in a location, the methodologies for estimating future SR scenarios can vary. In this section, methodologies for 3 cases are discussed (Fig. 1).

1.1. Case 1: measured SR is available

When measured SR is available for a location, future scenarios are derived using several downscaling methodologies that transfer the large-scale GCM output to a local scale using (1) analogies with different climatic zones or historical time periods, (2) simple manipulation of current climate observations (e.g. delta change factor methodology, DM), and (3) more sophisticated statistical and dynamical downscaling methodologies.

In DM, the arithmetic difference (ratio) between a GCM variable derived from a current climate simulation and that derived from a future climate scenario at the same GCM grid location is calculated. This difference (ratio) is then added (multiplied) to the observed local values to obtain the modeled future values (Anandhi et al. 2011). In the dynamic downscaling approach, an RCM is nested into a GCM (Uno et al. 2012, Yoshida et al. 2012). Statistical downscaling involves developing quantitative relationships between
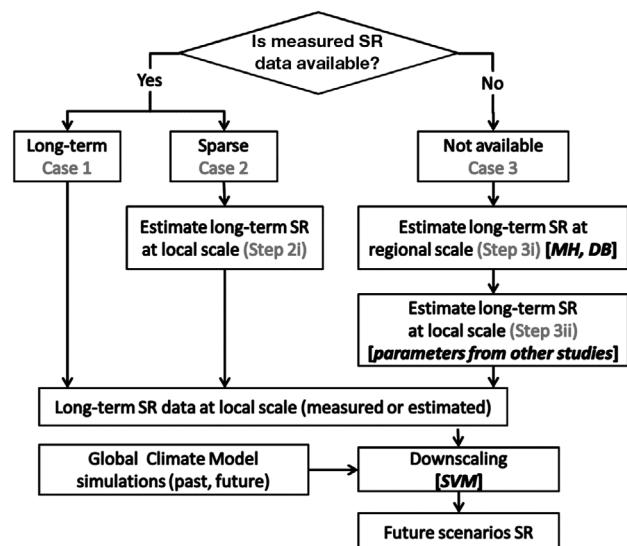

Fig. 1. Schematic representation to estimate future scenarios of solar radiation (SR). Long-term: >25 yr long record of monthly SR time series; local scale: a single site; regional scale: area-mean across sites. The methods/techniques used in this study are noted in italics. For further abbreviations see Table 1

the large-scale atmospheric variables (predictors) and the local surface variables (predictands). There are 3 types of statistical downscaling: weather classification methods, weather generators, and transfer functions. Weather classification methods group days into a finite number of discrete weather types or 'states' according to their synoptic similarity (Lamb 1972, Wetterhall et al. 2005, Anandhi 2010). Weather generators are stochastic models of observed sequences of weather variables (Mehrotra et al. 2006, Chen et al. 2010). The transfer functions capture the relationships between the predictors and the predictands (Schoof et al. 2007, Iizumi et al. 2008). Transfer functions that have been used in the recent past include linear and nonlinear regression, ANNs, canonical correlation analysis, PCA, and SVMs. Good reviews on downscaling methods can be found in Wilby et al. (2004), Fowler et al. (2007), and Maraun et al. (2010).

1.2. Case 2: measured SR available but sparse

When measured SR is sparse for a location, an additional step is required before methodologies that are applicable to Case 1 can be used to estimate future SR scenarios. This additional step (Step 2i in Fig. 1) involves estimating the SR at the local scale using methods that are available in the literature (some are discussed here). Then the future SR scenarios are derived by transferring the GCM's simulated large-scale information to a local scale using the downscaling methodologies employed in Case 1.

A number of techniques have been used to overcome the problems associated with using sparse data. The gaps between the needs and availability of SR data are filled in several ways: (1) using global datasets as a substitute for local data, (2) combining spatially coarse but temporally complete global datasets with spatially fine but temporally limited measured local data, (3) estimating SR from other measured meteorological variables using physical and empirical approaches, and (4) deriving data based on information from satellites (Deng et al. 2010, Chen et al. 2011, Iizumi et al. 2012, Wu & Liu 2012). Each of these methods has its own set of advantages and pitfalls. Some of the techniques that were used in the past to estimate SR in data-sparse areas include: (1) regression models and Bayesian approaches, which combine spatially coarse but temporally complete global datasets, and spatially fine but temporally limited measured local data to estimate the local SR in a manner that incorporates the space-time dynamics. The limitation with this meth-

od is that the grid interval of global datasets is too coarse to identify the local weather conditions at a site, and there are uncertainties in the grid-point values (Iizumi et al. 2012) due to the amount of representative measured data available for the region. (2) Satellite-based RS methods are another possibility; they estimate SR from variable(s) (e.g. land surface temperature) that are derived based on the thermal radiation emitted by the earth. The advantages of this method are that it is quick and reliable in data processing, practical to derive data for inaccessible or remote regions (mountainous and rural), and easy to manipulate the data with a computer (Şahin et al. 2013). However, absence of a long-term (>25 yr) satellite database is a limitation of this method. (3) Finally, empirical relationships and soft computing techniques (e.g. ANNs, SVMs) can be used to estimate SR at a location from other measured meteorological variables (e.g. sunshine duration, maximum and minimum air temperatures, relative humidity, precipitation). The sunshine-based method is generally more accurate, and, in its absence, air temperature-based methods are commonly used because temperature is more routinely measured at most meteorological stations (Chen & Li 2012). The ratio of the meteorological stations recording SR to those recording temperature is about 1:500 around the world (Chen et al. 2011). The parameters of these empirical formulae need to be estimated and tested locally for accuracy. Good reviews of empirical models to estimate SR are available in Menges et al. (2006) and Katiyar & Pandey (2013).

1.3. Case 3: measured SR not available

When measured SR data are not available, 2 additional steps (Steps 3i and 3ii; Fig. 1) are required, before using the methodologies applicable to Cases 1 and 2 to estimate future SR scenarios. The first step (Step 3i; Fig. 1) involves estimating the SR in the surrounding regions which have completely or sparsely measured records of SR using methods that are discussed in Case 1 or 2. In the second step (Step 3ii), using the calibrated parameters from regions having measured records, the parameters for a location with no measurements are estimated using one of the following approaches: (1) an indirect approach of model parameter regionalization using characteristics (e.g. climate, altitude, latitude, and longitude), (2) solving as an inverse problem providing the localized values of parameters meeting the needs of the regionalized specific model (e.g. a linear or nonlinear regression)

(Cheng et al. 2006), and (3) using parameters from earlier studies.

In all 3 cases, the long-term SR at a local scale is obtained (estimated or measured) using the methodologies provided. Future SR scenarios are then obtained by downscaling the simulations from GCMs or RCMs to the long-term SR (Fig. 1).

2. DESCRIPTION OF THE CASE STUDY

2.1. Study region

In this study, data from the MRB located in southern India were used to demonstrate the methodology in Case 3. The Malaprabha reservoir catchment (MC) is a semi-arid region with an area of 2564 km^2 (Fig. 2). The Malaprabha reservoir is the main source of water for irrigation, domestic, and industrial uses in a region with 3 million people — the 4 districts of northern Karnataka (George et al. 2008). The Malaprabha reservoir supplies irrigation water for an area of 218 191 ha in northern Karnataka. However, intense agricultural practices and the absence of reasonable water resource management have led to an unmet increase in water demand.

The climate of the study region can be broadly classified into 2 seasons based on precipitation: a wet season (the monsoon season) and a dry season. Downscaling of cloud cover was done to account for the 2 distinct climate conditions in the study area. For this purpose, the precipitation-based wet and dry seasons identified in an earlier study (Anandhi et al. 2008) were adopted in this study.

2.2. Data used

The reanalysis data of atmospheric variables for the study region from the NCEP (Kalnay et al. 1996) were extracted at monthly scale for the period of January 1978 through December 2000. The atmospheric variables were extracted for 9 grid points whose latitudes ranged from 12.5° to 17.5° N and longitudes ranged from 72.5° to 77.5° E, at a spatial resolution of 2.5°.

The monthly GCM data used in the study were extracted from simulations by the CCCma's third-generation CGCM3 (Kim et al. 2002) for the present-day climate (20C3M) and for 4 emission scenarios specified in the SRES (Nakicenovic et al. 2000), namely, A1B, A2, B1, and COMMIT. The GCM data were re-gridded to a common 2.5° NCEP grid by bilinear interpolation using GrADS (Doty & Kinter

1993). The baseline period in the study was 1978–2000, while the future time period was 2001–2100.

The average monthly CC and maximum and minimum air temperature data were estimated for the study region using daily records available from a gauging station located in Gadag (15°25′N, 75°38′E) for the period of January 1978 through December 2000 (Fig. 2). The weather station is maintained by the India Meteorological Department.

2.3. Estimating SR from meteorological variables

SR at a local scale was estimated using MH (Supit & van Kappel 1998) and DB (Donatelli & Bellocchi 2001) methods. More details on these methods are provided in Supplement 1 at www.int-res.com/articles/suppl/c059p259_supp.pdf. These methods use measured meteorological variables (temperature and CC) and the parameters listed in Section 3.1. The parameter values for these models were taken from other studies (Donatelli & Bellocchi 2000, Biggs et al. 2007) covering the MRB. The proposed methodology for Case 3 for estimating SR in the absence of measured data was tested with the satellite measurements provided by Biggs et al. (2007) for the region. Their study obtained SR from NASA's SRB Release 2 at 1° resolution from March 1984 to September 1995.

The sensitivity of different parameters used in SR estimation methods (DB and MH) was assessed by perturbing each parameter one-at-a-time (Morris 1991) about a fixed percentage (−100 % to +100 %, with increments of 20 %). The parameters considered in this study were those found in the DB method, τ, b, c_1, and c_2 representing the clear sky transmissivity, temperature range coefficient, and first and second seasonality factors, respectively. A_s, B_s, and C_s/R_{exo} are Hargreaves site-specific coefficients obtained by multiple linear regression. The most sensitive parameters were chosen for model calibration. During the calibration, the parameters which provided the least RMSE (the best fit) were selected. Using these parameters, the model was validated. SR was estimated using this validated model.

2.4. Downscaling temperatures and CC using SVMs

SVM, a novel machine learning tool popular for predicting SR (Deng et al. 2010, Chen et al. 2011), was used in this study as it was found to be effective for downscaling meteorological variables (Anandhi
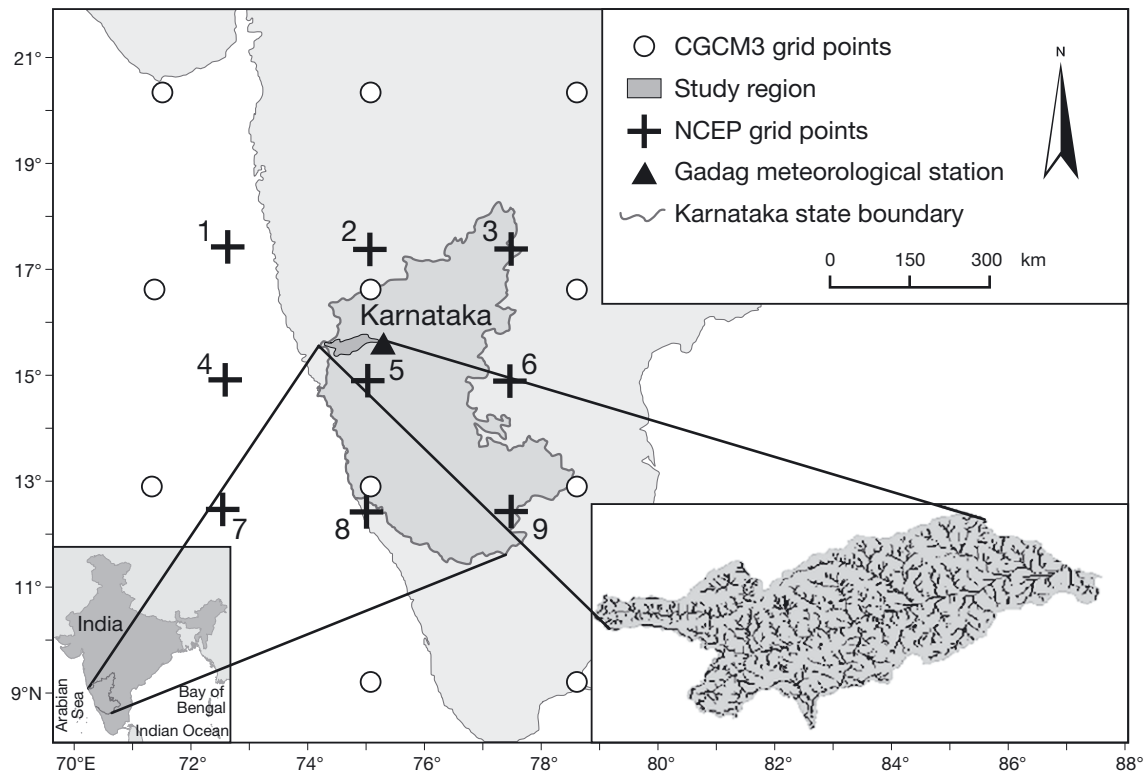
Fig. 2. Study region (Malaprabha reservoir catchment) in the state of Karnataka, India. The data extracted at CGCM3 grid points are re-gridded to the nine 2.5° NCEP grid points

et al. 2008, 2009, 2012). The future projections of SR were estimated using the downscaled values of future CC and maximum and minimum air temperatures at a local scale. The basic concept of SVM is to map input data into a higher dimensional feature space, and further to employ linear regression in the feature space (Vapnik 1998). More detailed information on SVM is available in Vapnik (1995) and Vapnik (1998). The SVM has the advantage of implementing the structural risk minimization principle, and is based on statistical learning theory (Deng et al. 2010). Further, it has the theoretical ability to learn any training set without error. Furthermore, the global optimum solution is possible with SVM (Chen et al. 2011). The main disadvantages of SVM algorithms are their large memory requirements and the extensive computational time needed to deal with very large datasets (Zhang et al. 2005). Further explanations on developing the downscaling model using SVM can be found in Anandhi et al. (2008, 2009, 2012) and Supplement 2 at www.int-res.com/articles/suppl/c059p259_supp.pdf. In the past, very few studies have statistically downscaled daily CC (Enke & Spekat 1997, Wilby et al. 1998). In this study, SVM was used for the first time to downscale CC.

2.5. Steps in downscaling using SVMs

The steps involved in developing each of the SVM models (Fig. 3) for downscaling were as follows:

Step 1: Select probable predictors at each of the NCEP grid points surrounding the study region. The choice of predictors could vary with region, season, and the predictand to be downscaled. More information on predictor selection can be obtained from Anandhi et al. (2012). The selected probable predictors used in this study are given in Table 2, pertaining to 9 grid points within and around the study region.

Step 2: Prepare scatter and correlation plots corresponding to each grid point using 3 measures of dependence (Pearson's product moment correlation and nonparametric rank correlations, namely Spearman's rho and Kendall's tau explained in Anandhi et al. 2008) between predictor variables in NCEP and GCM datasets, and between predictor variables in NCEP data and predictand.

Step 3: Select highly correlated predictors (potential predictors) by specifying 2 thresholds: T_{ng} and T_{np}. T_{ng} represents the threshold for correlation between predictor variables in NCEP and GCM datasets, and T_{np} represents the threshold for corre-
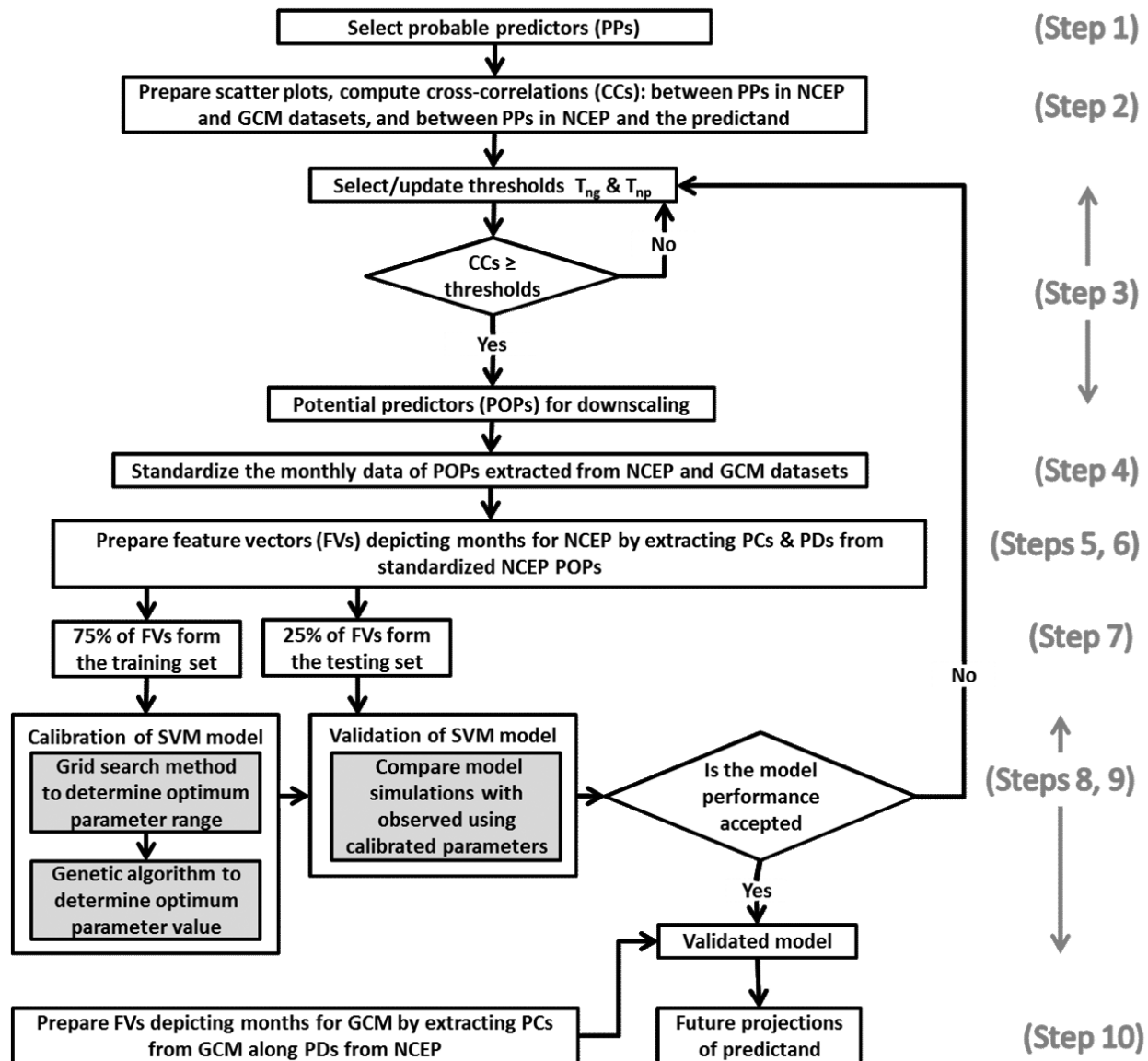
Fig. 3. Methodology followed for support vector machine (SVM) downscaling. PCs and PDs: principal components and principal directions, respectively; T_{ng}: the threshold for correlation between predictors in NCEP and GCM datasets; T_{np}: the threshold for correlation between predictors in NCEP data and the predictand; other abbreviations as in Table 1. Steps 1 to 10 in the figure are explained in Section 2.5

lation between predictor variables in NCEP data and predictand. Potential predictors are selected for each grid point, while the probable predictors are common to all the grid points. For example, to downscale air temperature, one of the probable predictors is Ta 925 at all 9 grid points, while potential predictors are Ta 925 values at selected grid points (2, 3, 5, and 6).

Step 4: Standardize the potential predictors for the baseline period (1978–2000) to reduce systemic bias (if any) in the mean and variance of the predictors in the GCM data, relative to those of the predictors in the NCEP reanalysis data. This step typically in-

volves subtraction of the mean and division by the SD of the predictor for the period.

Step 5: Analyze the PCs of standardized NCEP predictor data to extract PCs that are orthogonal and preserve >98% of the variance in the data. The PCs of GCM predictor data are extracted along the principal directions of NCEP predictor data. The PCs account for most of the variance in input, reduce the dimensionality of the data and also remove the correlations, if any, among the input data. They make the model more stable and reduce the computational load.

Step 6: Prepare for feature vectors using PCs. The PCs for each month are a feature vector and are inputs to the SVM model. The contemporaneous value of the predictand is its output.

Step 7: Partition feature vectors into a training set (calibration) and a testing set (validation); 70% of the feature vectors are used for training the SVM model, and the remaining 30% are used for validation of the developed model.

Step 8: Calibrate the SVM model to determine parameters, namely kernel width (σ) of RBF and penalty term C, during training of the model. In this study, we used a grid search procedure (van Gestel et al. 2004) to find the optimum range for each of these 2 parameters. Subsequently, the optimum values of the parameters are obtained from among the selected ranges using the stochastic search technique of a genetic algorithm (Haupt & Haupt 2004).

Step 9: Validate the developed SVM model using feature vectors in the testing set as input to the calibrated model, and compare output with the contemporaneous values of the observed predictand. We used the NMSE as an index to assess the performance of the model (Zhang & Govidaraju 2000).

Step 10: Obtain future projections of the predictand using feature vectors prepared from GCM simulations for the 2001–2100 period as input to the validated SVM downscaling model for each of the 4 emission scenarios (A1B, A2, B1, and COMMIT).

Step 11: Conduct trend analysis on SR estimated from downscaled meteorological variables over the period 1978–2100 using Sen's slope (Sen 1968) and Mann-Kendall tau (Helsel & Hirsch 1992) methods that are described in Supplement 3 at www.int-res.com/articles/suppl/c059p259_supp.pdf.

3. RESULTS

3.1. Sensitivity of SR estimation methods to changes in parameters

The estimated SR values for various perturbations of the 4 parameters (τ, b, c_1, and c_2) in the DB method are provided in Fig. 4a, while those of 3 parameters (A_s, B_s, and C_s/R_{exo}) in the MH method are provided in Fig. 4b. From Fig. 4a, it can be observed that the variability in the estimated SR for perturbations in τ was the highest, and was therefore considered the most sensitive parameter. It was followed by the b, c_1, and c_2 parameters in the DB method. In the MH method (Fig. 4b), B_s was the most sensitive parameter, followed by C_s/R_{exo} and A_s. It was also observed that in most cases the SR estimated by the DB method was lower than that estimated by the MH method for the different parameter perturbations considered. Sensitive parameters were calibrated.

3.2. Estimated SR

The calibrated parameter values in the MH method were $A_s = 0.045$, $B_s = 0.20$ and $C_s/R_{exo} = 0.14$. The calibrated parameters in the DB method τ, b, c_1, and c_2 were 0.6900, 0.0846, 0.0290, and 0.0080, respectively. Using these parameters, measured maximum and minimum air temperatures and CC at Gadag station, SR was estimated for the study region.

The proposed methodology in Case 3 (estimating SR in the absence of measured data) was validated by comparison with the observed data for the region from Biggs et al. (2007) (Fig. 5). The observed data
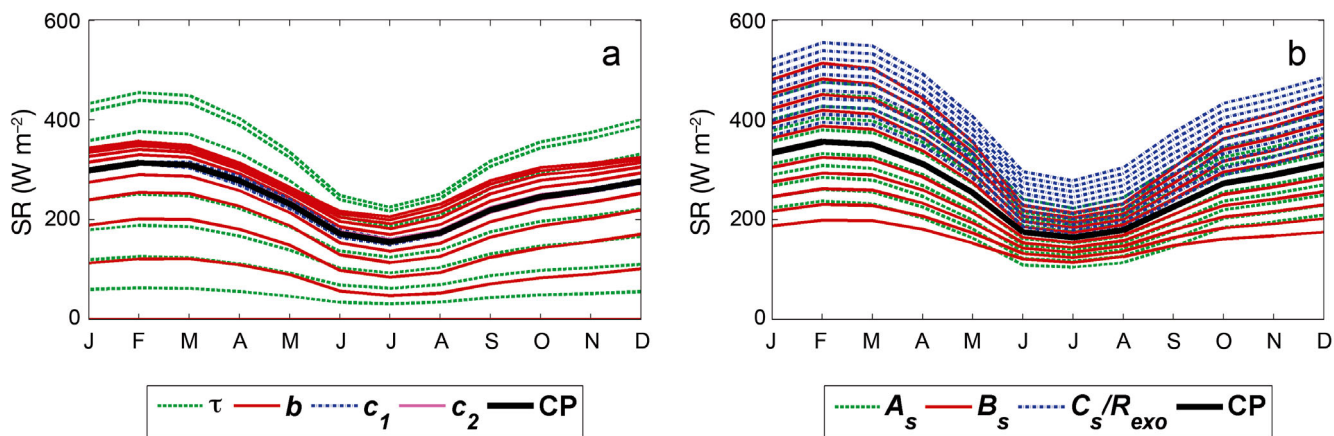

Fig. 4. Variability in the estimated solar radiation (SR) for perturbations in (a) 4 input parameters in the Donatelli-Bellocchi method and (b) 3 input parameters in the modified Hargreaves method. CP: solar radiation estimated using calibrated parameters; τ: clear sky transmissivity; other parameters defined in Section 2.3
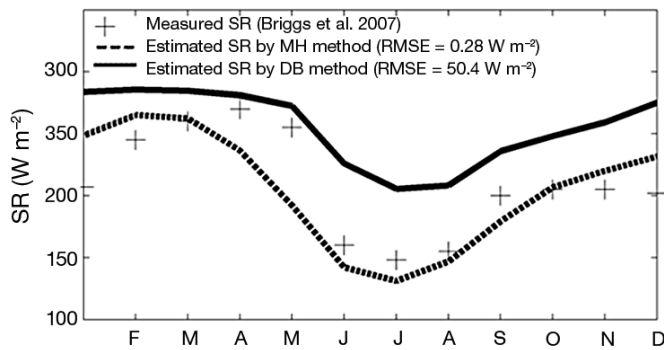
Fig. 5. Mean monthly solar radiation (SR) at latitude 15.5° N estimated using the Donatelli-Bellocchi (DB) and modified Hargreaves (MH) methods for the period 1978–2000 and measured SR from Biggs et al. (2007)

was for the period March 1984 to September 1995, while the modeled data was for the period 1978–2000. From the figure, it can be observed that the differences between measured and estimated SR values were relatively small during the April–May (June–November) period for the DB (MH) method, and the corresponding RMSE was 50.4 W m^{-2} (28 W m^{-2}). The SR fluxes estimated with the DB method were consistently higher than those estimated with the MH method.

3.3. Downscaling of maximum and minimum air temperatures

As part of an earlier study, the authors had already downscaled IPCC scenario–based maximum and minimum temperatures for the study area. More details on this work are available in Anandhi et al. (2009). The potential predictors selected are provided in Table 2. The downscaled maximum and minimum air temperatures were projected to

Table 2. Probable predictors (selected from NCEP and CGCM3 monthly datasets) for downscaling predictands. See Table 1 for abbreviations

	Predictand	Probable predictors
1	Maximum temperature	Ta 925, Ua 925, Va 925, LH, SH, SWR, LWR
2	Minimum temperature	Ta 925, Ua 925, Va 925, LH, SH, SWR, LWR
3	Cloud cover	PRW

increase in the future for A1B, A2, and B1 scenarios, whereas no trend was discerned for the COMMIT scenario. The projected increase in maximum and minimum air temperatures was high for the A2 scenario, and it was least for the B1 scenario.

3.4. Downscaling of CC

The CC was downscaled in this study for use in SR estimation. The amount of PRW, a large-scale atmospheric variable and a predictor for the seasonal component of radiation (Iizumi et al. 2008), was the probable predictor for downscaling CC. More PRW in the atmosphere indicates more moisture, which causes a statically unstable atmosphere leading to more vigorous overturning that results in more precipitation. An increase in the likelihood of precipitation indicates more cloudiness.

To verify the reliability of the PRW simulations by the GCM and to study the predictor–predictand relationships, we prepared scatter plots and computed cross-correlation using information for each of the 9 NCEP grid points enclosing the study area and their collective information. The plots between the PRW in NCEP and GCM datasets (Fig. 6) show that the predictor variable was realistically simulated by the GCM. Furthermore, the plots between the PRW in NCEP data and the observed CC (Fig. 7a,b) show that the PRW was positively correlated with the CC. Thus, the PRW at 1–9 grid points were selected as potential predictors.

The optimal values of the SVM parameters, i.e. kernel width (σ) and penalty term (C) were 50 and 4050, respectively. The downscaled CC values were compared with the observed values (Fig. 7) for calibration and validation periods and for wet and dry seasons. The results showed good correlation between the SVM downscaled CC and the observed CC with an NMSE of 0.33 and 0.43 for wet and dry seasons, respectively.

This study showed that CC is expected to increase in the future for A1B, A2, and B1 scenarios, whereas no trend was discerned for the COMMIT scenario. The projected increase in CC was relatively high for the A2 scenario, and it was least for the B1 scenario.

3.5. Trend in the SR projections

The trend was analyzed for the SR estimated by the MH method for the various IPCC scenarios using Sen's slope and the Mann-Kendall method for the
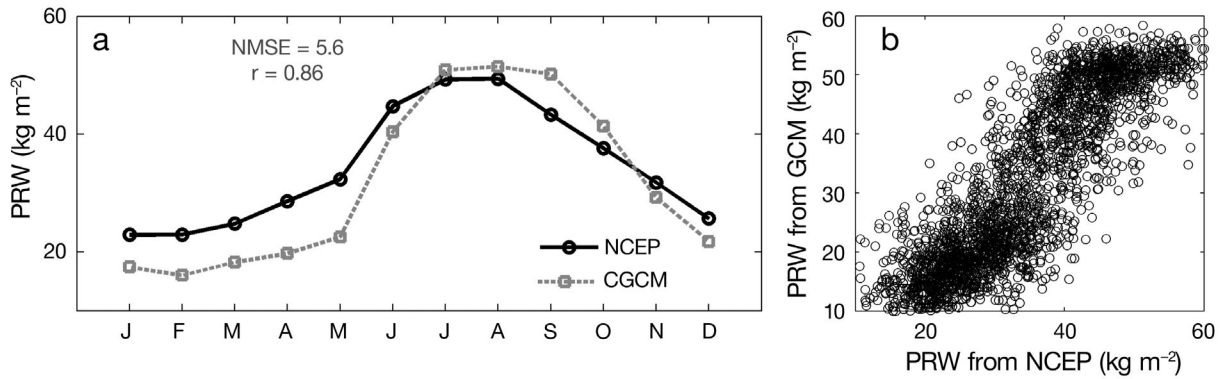
Fig. 6. (a) Monthly mean and (b) scatter plots prepared to verify the reliability of the simulation of the precipitable water (PRW) by the global climate model. r and NMSE: the linear correlation and normalized mean square error, respectively, between PRW in NCEP and CGCM3 datasets. Other abbreviations in Table 1
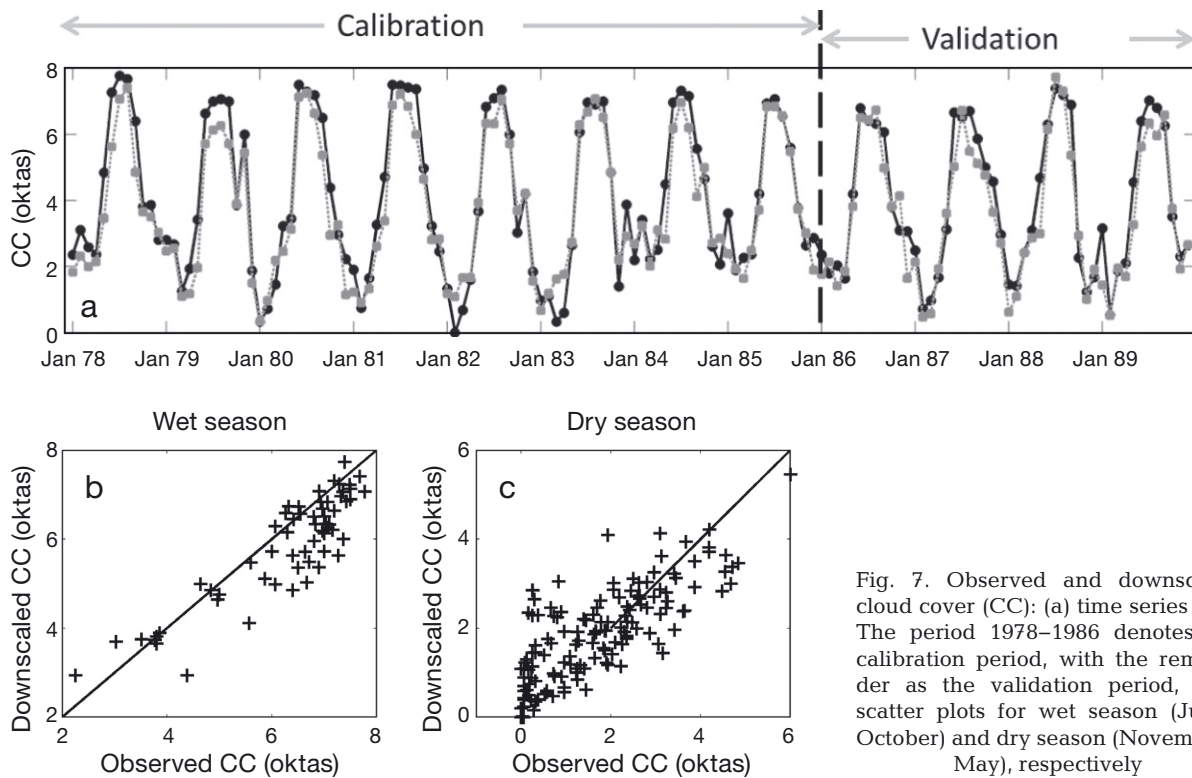

Fig. 7. Observed and downscaled cloud cover (CC): (a) time series plot. The period 1978–1986 denotes the calibration period, with the remainder as the validation period, (b,c) scatter plots for wet season (June–October) and dry season (November–May), respectively

period 1978–2100. For the baseline period (1978–2000), the study region had a decreasing trend of -2.7 W m^{-2} decade^{-1} and was not statistically significant (Fig. 8a).

The projected scenarios of SR projections for each of the 4 emission scenarios (A1B, A2, B1, and COMMIT) were estimated using MH methods (described in Section 2.5). Estimated SR was found to decrease in the future for A1B, A2, B1, and COMMIT scenarios. Among the 4 scenarios, the slope was steepest for the A2 scenario (-1.2 W m^{-2} decade^{-1}), followed by A1B (-1.0 W m^{-2} decade^{-1}), B1 (-0.4 W m^{-2} decade^{-1}), and COMMIT (no change) scenarios (Fig. 8b–e), at the 99 % significance level. The projected decrease in SR was higher for the A2 scenario (12.2 W m^{-2} yr^{-1}), whereas it was least for the COMMIT scenario (0.4 W m^{-2} yr^{-1}) (Fig. 8b). SR simulations downloaded directly from the CGCM3 model also showed decreasing trends in the future for these 4 scenarios (Figs. S1–S4 in Supplement 1).
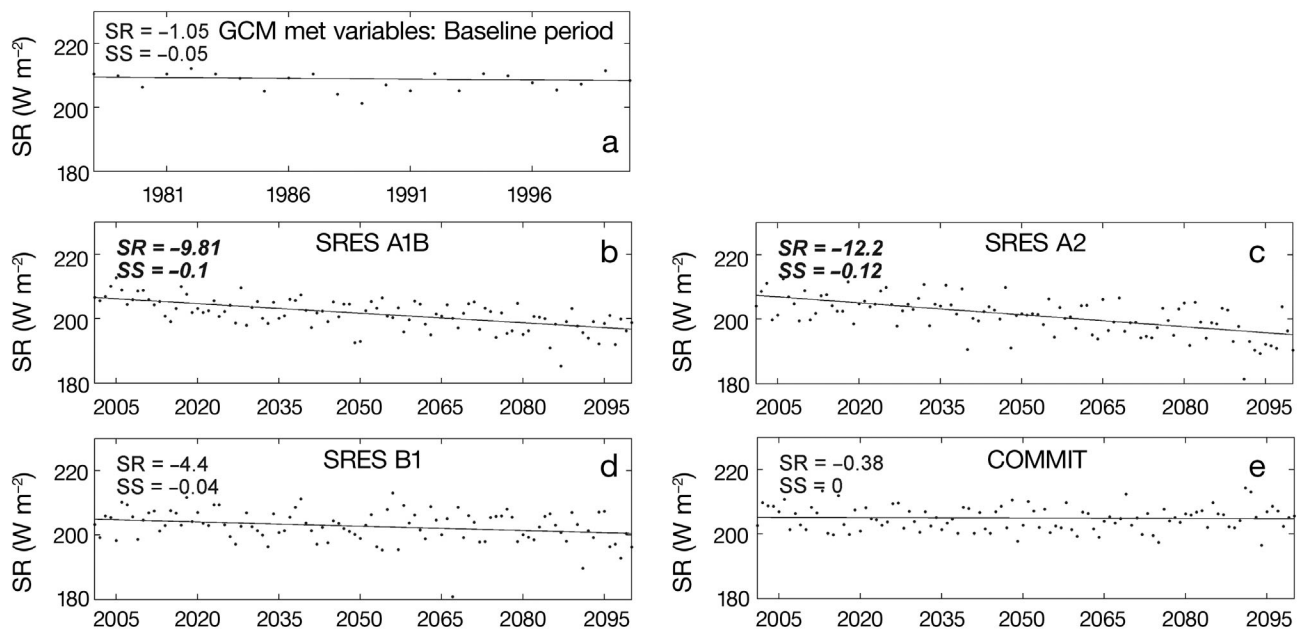
Fig. 8. Trend analysis in the estimated rate of change in solar radiation per year (SR) using Sen's slope method (a) for the baseline period 1978–2000 and (b–e) for the future period 2001–2100 for the 4 emission scenarios. SR was estimated using the modified Hargreaves method. SS: Sen's slope value (W m^{-2} yr^{-1}). **Bold italics**: significant changes

4. DISCUSSION

In estimation of SR using MH and DB methods, the parameters were calibrated. The calibrated parameters were comparable to those from earlier studies. In the study by Biggs et al. (2007), the parameter values in the entire Krishna basin estimated by using the MH method were $A_s = 0.045$, $B_s = 0.20$, and $C_s/R_{exo} = 0.15$. The parameters in the DB method obtained from SIPEAA (2004) for Hyderabad were 0.69, 0.0846, 0.029, and 0.008 for τ, b, c_1, and c_2, respectively.

The trends in CC are consistent with the results from an earlier study. The increase in precipitation in the region (Anandhi et al. 2008), increases the CC and, in turn, decreases the SR (Iizumi et al. 2008). Spatially variable changes in annual CC were observed in the region surrounding the basin (Biggs et al. 2007).

The decreasing trend in SR was in agreement with that reported in previous studies, showing a decrease in SR during the period 1952–2001 in India (Biggs et al. 2007, Wild 2009). In this region, changes in cloudiness and anthropogenic aerosol forcing were found to be the cause of decreasing SR (Biggs et al. 2007). Further, the decreasing trend in the simulated diurnal temperature range was translated to a decreasing trend in SR through the MH model.

5. SUMMARY AND CONCLUSIONS

In this study, we briefly discussed 3 different methodologies for estimating future scenarios of SR, namely: Case 1: SR is measured, Case 2: SR is measured but sparse, and Case 3: SR is not measured. In Case 1, future scenarios were derived using downscaling methodologies that transfer the simulated large-scale information of GCMs to the local scale (measurements). In Case 2, the long-term SR was first estimated at the local scale using sparse measured records, and then future scenarios were derived using several downscaling methodologies. While in Case 3, the long-term SR was first estimated at the regional scale, which has completely or sparsely measured records of SR, from which SR at the local scale was estimated. Finally, the future scenarios were derived using downscaling methodologies.

Implementation of the methodology provided in Case 3 to estimate SR scenarios for regions with no SR data was successfully demonstrated by applying it to a concrete example, i.e. the Malaprabha River basin in southern India. Calibration and validation results indicated that the performance of the methodology and downscaling of meteorological variables with SVM were satisfactory. The future SR scenarios obtained using the methodology were dependent on

the availability of observed data on predictor (meteorological) variables, choice of models/methods used in estimating SR, model parameter sensitivity, future emission scenario, downscaling methods, and GCMs. To bring out the variability in the future scenarios of SR, 4 emission scenarios (A1B, A2, B1, and COMMIT) from the CGCM3 were considered in this study.

The results of future scenarios of meteorological variables (predictors of SR) in the study area indicated that the maximum and minimum temperatures and CC are projected to increase in the future under the A1B, A2, and B1 scenarios. The projected increase was high for the A2 scenario, whereas it was least for the B1 scenario. The results of future scenarios of SR estimated based on downscaled CC and temperatures revealed that SR was projected to decrease in the future for the A1B, A2, B1, and COMMIT scenarios. The decrease was the highest for the A2 scenario and least for COMMIT. More model simulations are needed to explain the reductions in estimated future solar radiation.

LITERATURE CITED

Anandhi A (2010) Assessing impact of climate change on season length in Karnataka for IPCC scenarios. J Earth Syst Sci 119:447–460

Anandhi A, Srinivas VV, Nanjundiah RS, Kumar DN (2008) Downscaling precipitation to river basin in India for IPCC SRES scenarios using support vector machine. Int J Climatol 28:401–420

Anandhi A, Srinivas VV, Kumar DN, Nanjundiah RS (2009) Role of predictors in downscaling surface temperature to river basin in India for IPCC SRES scenarios using support vector machine. Int J Climatol 29:583–603

Anandhi A, Frei A, Pierson DC, Schneiderman EM, Zion MS, Lounsbury D, Matonse AH (2011) Examination of change factor methodologies for climate change impact assessment. Water Resour Res 47:W03501, doi:10.1029/2010WR009104

Anandhi A, Srinivas VV, Kumar DN, Nanjundiah RS (2012) Daily relative humidity projections in an Indian river basin for IPCC SRES scenarios. Theor Appl Climatol 108:85–104

Biggs T, Scott C, Rajagopalan B, Turral H (2007) Trends in solar radiation due to clouds and aerosols, southern India, 1952–1997. Int J Climatol 27:1505–1518

Chen J, Brissette FP, Leconte R (2010) A daily stochastic weather generator for preserving low-frequency of climate variability. J Hydrol (Amst) 388:480–490

Chen JL, Li GS (in press) Estimation of monthly mean solar radiation from air temperature in combination with other routinely observed meteorological data in Yangtze River basin in China. Meteorol Appl, doi:10.1002/met.1306

Chen JL, Liu HB, Wu W, Xie DT (2010) Estimation of monthly solar radiation from measured temperatures using support vector machines—a case study. Renew Energy 36:413–420

Cheng Q, Ko C, Yuan Y, Ge Y, Zhang S (2006) GIS modeling for predicting river runoff volume in ungauged drainages in the greater Toronto area, Canada. Comput Geosci 32:1108–1119

Deng F, Su G, Liu C, Wang Z (2010) Prediction of solar radiation resources in China using the LS-SVM algorithms. Computer and Automation Engineering (ICCAE), 2010. In: 2nd Int Conf, Singapore 26–28 February 2010, Singapore, p 31–35, doi:10.1109/iccae.2010.5451535

Donatelli M, Bellocchi G (2000) RadEst3: software to estimate global solar radiation. In: Proc 3rd Int Crop Sci Congr Eur Soc Agron 17–22 Aug, Hamburg

Donatelli M, Bellocchi G (2001) Estimate of daily global solar radiation: new developments in the software. In: Bindi M, Donatelli M, Porter JR, van Ittersum MK (eds) Proc 2nd Int Symp Model Crop Syst 16–18 July, Florence, p 213–214

Doty B, Kinter JI (1993) The grid analysis and display system (grads): a desktop tool for earth science visualization. American Geophysical Union 1993 Fall Meeting, San Fransico, CA, 6–10 December

Enke W, Spekat A (1997) Downscaling climate model outputs into local and regional weather elements by classification and regression. Clim Res 8:195–207

Fowler HJ, Blenkinsop S, Tebaldi C (2007) Linking climate change modeling to impacts studies: recent advances in downscaling techniques for hydrological modeling. Int J Climatol 27:1547–1578

George B, Malano HM, Davidson B (2008) Water resource allocation modelling to harmonise supply and demand in the Malaprabha catchment, India. In: Proc XIIIth World Water Congr, 1–4 September, Montpellier, p 1–14

Haupt R, Haupt S (2004) Practical genetic algorithm. John Wiley and Sons, Engelwood Cliffs, NJ

Helsel D, Hirsch R (1992) Statistical methods in water resources. Elsevier, Amsterdam

Iizumi T, Nishimori M, Yokozawa M (2008) Combined equations for estimating global solar radiation: projection of radiation field over Japan under global warming conditions by statistical downscaling. J Agric Meteorol 64:9–23

Iizumi T, Nishimori M, Yokozawa M, Kotera A, Duy Khang N (2012) Statistical downscaling with Bayesian inference: estimating global solar radiation from reanalysis and limited observed data. Int J Climatol 32:464–480

Kalnay E, Kanamitsu M, Kistler R, Collins W and others (1996) The NCEP/NCAR 40-year reanalysis project. Bull Am Meteorol Soc 77:437–471

Katiyar AK, Pandey CK (2013) A review of solar radiation models. I. J Renew Energy 2013:168048

Kim SJ, Flato G, Boer G, McFarlane N (2002) A coupled climate model simulation of the last glacial maximum. 1. Transient multi-decadal response. Clim Dyn 19:515–537

Lamb H (1972) British Isles weather types and a register of daily sequence of circulation patterns, 1861–1971, Vol 116. HMSO, London

Maraun D, Wetterhall F, Ireson AM, Chandler RE and others (2010) Precipitation downscaling under climate change: recent developments to bridge the gap between dynamical models and the end user. Rev Geophys 48:RG300

Mehrotra R, Srikanthan R, Sharma A (2006) A comparison of three stochastic multi-site precipitation occurrence generators. J Hydrol (Amst) 331:280–292

Menges HO, Ertekin C, Sonmete MH (2006) Evaluation of global solar radiation models for Konya, Turkey. Energy Convers Manag 47:3149–3173

Morris MD (1991) Factorial sampling plans for preliminary computational experiments. Technometrics 33:161–174

Nakicenovic N, Alcamo J, Davis G de Vries B and others (2000) IPCC special report on emissions scenarios. Cambridge University Press, Cambridge

Rivington M, Bellocchi G, Matthews K, Buchan K (2005) Evaluation of three model estimations of solar radiation at 24 UK stations. Agric For Meteorol 132:228–243

Şahin M, Kaya Y, Uyar M (2013) Comparison of ANN and MLR models for estimating solar radiation in Turkey using NOAA/AVHRR data. Adv Space Res 51:891–904

Schoof J, Pryor S, Robeson S (2007) Downscaling daily maximum and minimum temperatures in the USA: a hybrid empirical approach. Int J Climatol 27:439–454

Sen PK (1968) Estimates of the regression coefficient based on Kendall's tau. J Am Stat Assoc 63:1379–1389

SIPEAA (2004) Tools for agrometeorological and agricultural modelling. ISCI-CRA. www.sipeaa.it/ASP/ASP2/index_tools.asp

Supit I, van Kappel R (1998) A simple method to estimate solar radiation. Sol Energy 63:147–160

Teuling A, Hirschi M, Ohmura A, Wild M and others (2009) A regional perspective on trends in continental evaporation. Geophys Res Lett 36:L02404, doi:10.1029/2008GL036584

Uno F, Iizumi T, Nishimori M (2012) Time trends and variations in mean and accumulated solar radiation for the ripening period of paddy rice in Kyushu for 1979–2007. J Agric Meteorol 68:69–76

van Gestel T, Suykens JAK, Baesens B, Viaene S and others (2004) Benchmarking least squares support vector machine classifiers. Mach Learn 54:5–32

Vapnik V (1995) The nature of statistical learning theory. Springer, New York, NY

Vapnik V (1998) Statistical learning theory. Wiley, New York, NY

Wetterhall F, Halldin S, Xu C (2005) Statistical precipitation downscaling in central Sweden with the analogue method. J Hydrol (Amst) 306:174–190

Wilby R, Hassan H, Hanaki K (1998) Statistical downscaling of hydrometeorological variables using general circulation model output. J Hydrol (Amst) 205:1–19

Wilby R, Charles S, Zorita E, Timbal B, Whetton P, Mearns L (2004) Guidelines for use of climate scenarios developed from statistical downscaling methods. Supporting material of the Intergovernmental Panel on Climate Change, prepared on behalf of Task Group on Data and Scenario Support for Impacts and Climate Analysis (TGICA). http://ipccddc.cru.uea.ac.uk/guidelines/StatDownGuide.pdf

Wild M (2009) Global dimming and brightening: a review. Geophys Res Lett 114:D00D16, doi:10.1029/2008JD011470

Wu W, Liu HB (2012) Assessment of monthly solar radiation estimates using support vector machines and air temperatures. Int J Climatol 32:274–285

Yoshida R, Iizumi T, Nishimori M (2012) Inter-model differences in the relationships between downward shortwave radiation and air temperatures derived from dynamical and statistical downscaling models. J Meteorol Soc Jpn Ser II 90B:75–82

Zhang B, Govidaraju RS (2000) Prediction of watershed runoff using Bayesian concepts and modular neural network. Water Resour Res 36:753–762

Zhang JP, Li ZW, Yang J (2005) A parallel svm training algorithm on large-scale classification problems. In: Proc 2005 Int Conf on Machine Learning and Cybernetics, 18–21 August, Guangzhou. IEEE Vol 3, p 1637–1641